FEMS Microbiology Ecology, 91, 2015, fiv106

doi: 10.1093/femsec/fiv106
Advance Access Publication Date: 31 August 2015
Research Article

RESEARCH ARTICLE

Advancements in the application of NanoSIMS and Raman microspectroscopy to investigate the activity of microbial cells in soils

Stephanie A. Eichorst[1], Florian Strasser[1], Tanja Woyke[2], Arno Schintlmeister[1,3], Michael Wagner[1,3] and Dagmar Woebken[1,*]

[1]Division of Microbial Ecology, Department of Microbiology and Ecosystem Science, Research network 'Chemistry meets Microbiology', University of Vienna, Vienna 1090 Austria, [2]DOE Joint Genome Institute, Walnut Creek, CA 94598, USA and [3]Large-Instrument Facility for Advanced Isotope Research, University of Vienna, Vienna 1090 Austria

*Corresponding author: Division of Microbial Ecology, Department of Microbiology and Ecosystem Science, Research network 'Chemistry meets Microbiology', University of Vienna, Vienna 1090 Austria. Tel: +43-1-4277-76613; E-mail: woebken@microbial-ecology.net

One sentence summary: A procedure is presented that allows one to investigate the activity of soil microorganisms at the single-cell level by combining stable isotope-labeled substrate incubations with NanoSIMS or Raman microspectroscopy.

Editor: Max Häggblom

ABSTRACT

The combined approach of incubating environmental samples with stable isotope-labeled substrates followed by single-cell analyses through high-resolution secondary ion mass spectrometry (NanoSIMS) or Raman microspectroscopy provides insights into the *in situ* function of microorganisms. This approach has found limited application in soils presumably due to the dispersal of microbial cells in a large background of particles. We developed a pipeline for the efficient preparation of cell extracts from soils for subsequent single-cell methods by combining cell detachment with separation of cells and soil particles followed by cell concentration. The procedure was evaluated by examining its influence on cell recoveries and microbial community composition across two soils. This approach generated a cell fraction with considerably reduced soil particle load and of sufficient small size to allow single-cell analysis by NanoSIMS, as shown when detecting active N_2-fixing and cellulose-responsive microorganisms via $^{15}N_2$ and ^{13}C-UL-cellulose incubations, respectively. The same procedure was also applicable for Raman microspectroscopic analyses of soil microorganisms, assessed via microcosm incubations with a ^{13}C-labeled carbon source and deuterium oxide (D_2O, a general activity marker). The described sample preparation procedure enables single-cell analysis of soil microorganisms using NanoSIMS and Raman microspectroscopy, but should also facilitate single-cell sorting and sequencing.

Keywords: soil microorganisms; single-cell methods; NanoSIMS; Raman microspectroscopy; Nycodenz; stable isotopes

INTRODUCTION

Soils encompass an area of ca. 1.23×10^{14} m^2 on Earth (Whitman, Coleman and Wiebe 1998), which is home to a multitude of our planet's biodiversity including a vast number of bacterial, archaeal and fungal taxa. This microbial diversity is crucial for driving various biogeochemical cycles, yet our understanding of the participants and their activity remains rudimentary at best. The functions of microorganisms in soil have been extensively

Received: 4 June 2015; **Accepted:** 24 August 2015

studied on an ecosystem or community level with activity assays (Caldwell 2005) or in combination with stable isotopes (Radajewski, McDonald and Murrell 2003). Little attention, however, has been paid to the single-cell level that can provide valuable information on metabolic heterogeneity within a specific population (Huang *et al.* 2007; Lechene *et al.* 2007).

The incubation of environmental samples with stable isotope-labeled substrates followed by fluorescence *in situ* hybridization (FISH) (Wagner, Horn and Daims 2003; Amann and Fuchs 2008) and high-resolution secondary ion mass spectrometry (NanoSIMS) (Lechene *et al.* 2006) has been successfully applied to investigate the *in situ* function of (uncultivated) microorganisms in their native environment (Wagner 2009), such as freshwater and marine environments (including water columns and sediments) (Musat *et al.* 2008; Dekas, Poretsky and Orphan 2009; Halm *et al.* 2009; Foster *et al.* 2011; Morono *et al.* 2011; Ploug *et al.* 2011; Milucka *et al.* 2012) or microbial mats (Woebken *et al.* 2012; 2015). In soil systems, NanoSIMS has been mainly used to explore elemental and isotopic composition of soil organic and inorganic matter at the submicron scale (Hatton *et al.* 2012; Heister *et al.* 2012; Mueller *et al.* 2012; Remusat *et al.* 2012; Vogel *et al.* 2014) or in plant tissue and plant–fungi systems (Clode *et al.* 2009; Kilburn *et al.* 2010; Moore *et al.* 2011a,b; Nuccio *et al.* 2013; Kaiser *et al.* 2015). Microbial cells were observed in NanoSIMS investigations of a cultured bacteria–sand model system (Herrmann *et al.* 2007), but until now NanoSIMS has not been applied to specifically investigate the activity of bacteria or archaea in soil ecosystems.

Another single-cell technology, Raman microspectroscopy, is a rapid non-destructive vibrational spectroscopic method for obtaining information on the molecular composition of a sample (Huang *et al.* 2004; Jarvis and Goodacre 2004). It has been used as a whole-organism fingerprinting technique to distinguish bacteria (Rosch *et al.* 2005; Harz, Roesch and Popp 2009) or their life stages (Haider *et al.* 2010) based on their characteristic Raman spectra, or to identify storage compounds, pigments, cytochromes, etc. in individual microbial cells (Pätzold *et al.* 2008; Jehlicka, Edwards and Oren 2013; Kumar *et al.* 2015). When combined with FISH techniques, stable isotope tracer experiments and/or single-cell capturing methods, Raman microspectroscopy holds tremendous promise for assigning physiological function to uncultivated microorganisms as illustrated with naphthalene degradation (Huang *et al.* 2007), phenylalanine uptake (Haider *et al.* 2010), carbon dioxide fixation (Li *et al.* 2012) or as a general activity marker when combined with D_2O (Berry *et al.* 2015). As with NanoSIMS, Raman microspectroscopy has not been applied for single-cell investigations in soil systems, but has primarily been applied to classify soils and to characterize soil structure and/or mineral content (Corradob *et al.* 2008; Tomic, Makreski and Gajic 2010; Zheng *et al.* 2012; Luna *et al.* 2014).

The application of NanoSIMS and Raman microspectroscopy to the investigation of soil microorganisms is complicated by the dispersal of microorganisms within a high load of (background) soil particles. As such, the efficient application of both single-cell methods to the investigation of soil microorganisms would require a reduction of organic and inorganic background particle load and a concentration of the cells to yield a high cell density fraction. Thus, the detachment of cells from soil particles and subsequent cell concentration appears to be necessary to make soil microorganisms amenable for the aforementioned single-cell analyses. Previously, various physical (such as sonication) or chemical (such as detergents) cell detachment methods were applied to soils (Lindahl and Bakken 1995; Lindahl 1996; Barra Caracciolo *et al.* 2005; Bertaux *et al.* 2007; Holmsgaard *et al.* 2011), typically followed by density gradients with a solution of a higher density than microbial cells, such as Nycodenz (Rickwood, Ford and Graham 1982), to separate cells from particles. However, the efficiency of these methods is seldom compared across different soil types and is typically evaluated by assessing the total cell recovery (total number of extracted cells per gram soil), but not the effect on the microbial community structure [to our knowledge only (Holmsgaard *et al.* 2011) compared the starting and final community with next generation sequencing]. As such, the influence that these methods have on the microbial community structure and their compatibility with single-cell methods such as NanoSIMS and Raman microspectroscopy remains uncertain.

It was the aim of this study to develop a workflow for the efficient application of NanoSIMS and Raman microspectroscopy to soil microorganisms, and to assess the potential and limitations of stable isotope incubation experiments of soils in combination with these methods. Furthermore, the effects of typical physical and chemical cell detachment methods (as well as a novel combination of them) across two soil types were evaluated by analyzing the bacterial community structure and total cell recovery at various steps in the procedure. The developed preparation procedure of soil samples culminated in a concentrated cell fraction applicable for NanoSIMS and Raman microspectroscopy, as demonstrated by proof-of-concept soil microcosm experiments detecting active N_2-fixing (via $^{15}N_2$ incubations) and cellulose-responsive (via ^{13}C-UL-cellulose incubations) microorganisms by NanoSIMS and actively deuterium-incorporating cells (via D_2O incubations) by Raman microspectroscopy.

MATERIALS AND METHODS

Sample collection

Soil samples were collected at Klausen-Leopoldsdorf (beech forest soil) in Lower Austria and Neustift, Stubai Valley (alpine meadow soil) in the Austrian Central Alps. A description of the soils can be found in Table S1 (Supporting Information). Approximately three cores (8 cm diameter × 5 cm depth) were sampled per field replicate ($n = 3$ field replicates) to ensure robust statistical analysis (Prosser 2010). If there was a duff or plant litter layer present, it was brushed aside prior to the collection of the cores. Samples were stored at 4°C during the transport to the laboratory. The soil was homogenized by passage through a 2-mm sieve and an aliquot was frozen at –20°C (samples 'native soil').

Cell detachment and Nycodenz density gradient separation

Approximately 30 g of freshly collected soil were homogenized in 100 mL 1x phosphate-buffered saline (PBS) (pH 7.4) in triplicates (Fig. S1, Supporting Information). Upon homogenization, an aliquot per triplicate was archived at –20°C for DNA extractions (samples 'homogenized soil'). Furthermore, a 10 mL volume of this soil slurry from each technical replicate was aliquoted into a clean flask and the following treatments for cell removal were conducted: (1) 0.35% wt/v polyvinylpyrrolidone (PVP) (Sigma, St Louis, MO); and (2) 'combination treatment': combination of 0.5% v/v Tween 20, 3 mM sodium pyrophosphate (Sigma, St Louis, MO) and 0.35% wt/v PVP; (3) sonication for three 10-s pulses at a power setting of 60–65% with a

Sonoplus HD 2070 (Bandelin electronic, Berlin, Germany); and (4) 0.5% v/v Tween 20 (Sigma, St Louis, MO). The soil slurries were stirred at room temperature for 30 min to detach particle-associated cells. An aliquot was archived at –20°C for DNA extractions (samples 'cell detached soil') and the remainder was used for Nycodenz density gradient separation. The same procedure including the four different cell detachment treatments was also done with initially formaldehyde-fixed soil suspensions (from Klausen-Leopoldsdorf soil, final formaldehyde concentration of 4% (vol/vol)). The soil suspensions were fixed at room temperature for 1 h, washed with 1× PBS and resuspended in 1× PBS prior to the cell removal treatments.

For separation of cells from large soil particles and cell fraction collection, approximately 1 vol of the respective treated soil suspension was added to 1 vol of Nycodenz and centrifuged with a swing-out rotor on a Beckman Ultracentrifuge (rotor SWT14i) at 14 000 g for 90 min at 4°C (Barra Caracciolo *et al.* 2005), but using Nycodenz at 1.42 g mL^{-1} to better capture the microbial community as suggested previously (Laflamme *et al.* 2005; Holmsgaard *et al.* 2011) and also shown in our preliminary Nycodenz concentration testing results (Table S2, Data S1, Supporting Information). The entire aqueous upper layers were collected (Fig. S1, Supporting Information). An aliquot of the thoroughly mixed aqueous layer was filtered on polycarbonate filters (GTTP type, pore size 0.2 μm, Millipore, Billerica, MA) for DNA extractions (samples 'cell fraction'). Another aliquot was filtered on polycarbonate filters and total cell counts were performed using 4′,6-diamidino-2-phenylindole (DAPI) using standard methods. Cell recovery was analyzed for statistical differences using an analysis of variance with a Tukey's HSD mean separation using the R program version 2.13.1 (http://www.r-project.org/index.html).

16S rRNA gene amplicon sequencing and sequence analysis

To assess shifts in community structure due to the treatments and/or Nycodenz separation across the two soils, total DNA was extracted at various points during the cell detachment/separation protocol as indicated above (Fig. S1, Supporting Information) using the FastDNA® Spin Kit (MP Biomedicals, Solon, OH). For each DNA sample, 16S rRNA gene paired-end amplicon sequencing (iTags) was performed on the Illumina MiSeq platform at the Department of Energy Joint Genome Institute (Walnut Creek, CA) after PCR amplification targeting the hypervariable V4 16S rRNA gene region with 515F and 806R of both bacteria and archaea (Caporaso *et al.* 2011).

Sequence tags were trimmed, assembled and quality checked according to the JGI Illumina 16S rRNA gene amplicons (iTags) analysis pipeline as described in Caporaso *et al.* (2011). Briefly, contaminants, PhiX reads and unpaired reads were identified and discarded from the data set. Reads were trimmed to 165 bp and assembled with the FLASH software (Magoc and Salzberg 2011). Primer sequences were removed and sequences were further trimmed if the mean quality score was less than 30. The trimmed, assembled reads were filtered for additional quality; reads harboring more than 5 Ns and nucleotides quality score less than 15 were discarded. Filtered reads were clustered at 100% identity and clustered/denoised at 99% identity. Clusters harboring abundances lower than 3 were discarded and the remaining clusters were scanned for chimeras with UCHIME denovo and UCHIME reference (Edgar *et al.* 2011). OTUs were classified with the RDP classifier (Cole *et al.* 2005) supplemented with in-house training sets.

Additional diversity statistics and beta-diversity analysis were performed using the R program (http://www.r-project.org/index.html). Libraries were normalized to the smallest library [Klausen-Leopoldsdorf: $n = 32\,410$ (unfixed); $n = 9063$ (formaldehyde fixed) and Neustift: $n = 36\,880$ (unfixed)]. Bacterial richness, which is a measure of the number of different species, was estimated using Chao and Abundance Coverage Estimator at the operational taxonomic unit (OTU) of 0.03, which correlates to a sequence similarity of 97% (referred to as OTU_{97}). Bacterial diversity, which is a combined measure of the number of different species along with the relative abundance of those species, was estimated using the Shannon index at OTU_{97}. Furthermore, we evaluated changes in richness and diversity in the OTU_{97} clusters within specific phyla. Since FISH probes applied to highly diverse samples such as soils typically target a specific phylum, family or genus, the sequence data was evaluated at these taxonomic levels at a relative abundance detection limit of $\geq 0.1\%$ (previously reported as a reliable detection limit for the single-cell methods FISH; Amann and Fuchs 2008) to assess the effect of the developed sample preparation procedure on the community composition. To do so, the OTU_{97} clusters were grouped into phyla, families and genera based on the taxonomic classification from the RDP classifier (Cole *et al.* 2005) supplemented with in-house training sets (as described above); data were not reclustered at different OTU cut-offs, as the proper sequence similarity cut-off for genus, family and phylum is not conclusively defined. The number of phyla, families and genera present in the 'native soil' and final 'cell fraction' were counted. In addition, the number of phyla, families and genera gained and lost in the final 'cell fraction' were summarized. All data sets are publicly available through the JGI portal (http://genome.jgi-psf.org/Soisamitagplate1/Soisamitagplate1.info.html) and NCBI BioSample Accession Numbers can be found in Table S3, Supporting Information.

Soil microcosm incubations with ^{13}C-cellulose, $^{15}N_2$ or D_2O (proof of concept experiments)

^{13}C-cellulose microcosms consisted of approximately 6 g of Klausen-Leopoldsdorf soil in a 120-mL crimp-top vial supplemented with 12 mg of ^{13}C-UL-maize cellulose (99% atom; IsoLife, Wageningen, the Netherlands) amended with 10 mg of glucose. Control microcosms were non-supplemented with ^{13}C-UL-maize cellulose. Microcosms were incubated at room temperature (ca. 23°C) under low light conditions for 15 days and vented every 3 days to maintain an aerobic atmosphere.

$^{15}N_2$ microcosms consisted of approximately 2 g of soil from Klausen-Leopoldsdorf in a 12-mL crimp-top vial. Vials were sealed and the headspace was replaced with 80% $^{15}N_2$ (98% atom; Cambridge Isotope Laboratories, Cambridge, MA) and 20% oxygen. Control microcosms contained lab air. Control and $^{15}N_2$ microcosms were amended with 45 mg (500 μl of 0.5 M solution) of glucose and incubated at room temperature (ca. 23°C) under low light conditions for 21 days.

Deuterium oxide (D_2O) microcosms consisted of approximately 1 g of soil on top of a Whatman filter paper No. 1 (Sigma Aldrich, St. Louis, MO), cut to the circumference of the 120-mL crimp-top vial, which was supplemented with 200 μl of 100% D_2O (99.9 atm%, Sigma Aldrich, St. Louis, MO) or 200 μl of 0.14 M glucose in 100% D_2O. Prior to the establishment of the microcosms, the soil was dried at 37°C for approximately 45 min to half of its soil moisture in order to obtain a final D_2O concentration of 50% (vol/vol) upon the addition of the aforementioned supplements. Microcosms were sealed and incubated at room

temperature (ca. 23°C) under low light conditions for 13 days. Microcosms were re-supplemented with appropriate D_2O solution (50% D_2O (vol/vol)) every 3 days.

Soil cells from these microcosms were prepared for NanoSIMS (^{13}C-cellulose and $^{15}N_2$ incubations) and Raman microspectroscopy (^{13}C-cellulose and D_2O incubation) with the cell detachment/separation methods established in this study. Briefly, soil was fixed in 4% (vol/vol) formaldehyde for 1 h at room temperature and cells were detached from soil particles using the 'combination treatment' and separated on a Nycodenz density gradient as described above. Cell fractions (the upper layer of the Nycodenz gradient; Fig. S1, Supporting Information) were prepared for NanoSIMS or Raman microspectroscopy as described below.

NanoSIMS analysis

Cell fractions from the ^{13}C-cellulose and $^{15}N_2$ microcosm experiments were filtered onto a AuPd-coated polycarbonate filter (GTTP type, 0.2 μM pore size, Millipore, Billerica, MA), washed with 1x PBS and sterile water, air-dried and mounted onto the sample holder. NanoSIMS was performed at the Large-Instrument Facility for Advanced Isotope Research at the University of Vienna using a NanoSIMS 50L (Cameca, France). Prior to data acquisition, analysis areas were pre-sputtered utilizing a high-intensity Cs^+ primary ion beam to ensure that the analyzed regions were located within the cells. Data were acquired as images by scanning a finely focused Cs^+ primary ion beam (ca. 80 nm spot size) over areas between 20 × 20 and 50 × 50 μm^2. Images were recorded as multilayer stacks, each consisting of 5–15 individual cycles (i.e. layers). The carbon isotope composition was inferred from the signal intensities obtained from detection of $^{12}C^-$ and $^{13}C^-$secondary ions, and the nitrogen isotope composition was inferred from $^{12}C^{14}N^-$ and $^{12}C^{15}N^-$ secondary ions. Secondary electrons were detected simultaneously to secondary ions to facilitate target cell identification. Image data were evaluated using the WinImage software package provided by Cameca. Individual images were corrected for detector dead time and image drift from layer to layer prior to stack accumulation. Regions of interest (ROIs), referring to individual cells, were manually defined based on the CN^- secondary ion maps and cross-checked by the topographical/morphological appearance in secondary electron images. The isotopic composition for each ROI was determined by averaging over the individual images of the multilayer stack. Isotopic compositions are expressed as isotope fractions of the tracer content, i.e. $^{15}N/(^{14}N+^{15}N)$ and $^{13}C/(^{12}C+^{13}C)$) given in at%.

Amino acid/glucose labeling experiments

To test the influence of available amino acids in the environment on the applicability of the published 'red-shift' in the phenylalanine peak used for the detection of ^{13}C-enriched microorganisms by Raman microspectroscopy (Huang *et al.* 2004, 2007), we incubated extracted soil cells in a defined medium with varying concentrations of amino acids along with glucose at a final concentration of 10 mM. For this purpose, fresh soil samples were collected from the upper 5 cm from the sampling site at Klausen-Leopoldsdorf (beech forest soil) and ca. 30 g of 2-mm sieved soil was stirred at room temperature with 1x PBS supplemented with 35 mg polyvinylpyrrolidone in order to detach cells from soil particles. Cells were Nycodenz separated (1.42 g mL^{-1}) using the conditions described above. Approximately 30 cell fractions were pooled (total of ca. 150 mL) and the cell fraction was filtered on multiple polycarbonate filters (GTTP, pore size 0.2 μm, Millipore), which served as the source of inoculum.

The medium for growth experiments consisted of vitamins (excluding thiamine), inorganic salts and trace elements as described previously (Eichorst, Breznak and Schmidt 2007; Eichorst, Kuske and Schmidt 2011): VSB-5.5 (VSB- 'vitamins and salts base'; # indicates the respective pH of the basal solution). Approximately 10 mL of medium was added to sterile 120-mL crime-top vials in triplicate. There were two experimental permutations: (1) ^{13}C-amino acid mix with 10 mM ^{12}C-glucose and (2) ^{12}C-amino acid mix and 10 mM ^{13}C-glucose. The final amino acid concentrations were 1, 0.1, 0.001, 0.0001 and 0 g L^{-1}. Amino acid mixtures from algae [^{12}C- and ^{13}C-labeled (97–99% atom), Cambridge Isotope Laboratories, Tewksbury, MA] contained the following components (16 amino acids with approximate percentages): L-alanine (7%), L-arginine (7%), L-aspartic acid (10%), L-glutamic acid (10%), glycine (6%), L-histidine (2%), L-isoleucine (4%), L-leucine (10%), L-lysine (14%), L-methionine (1%), L-phenylalanine (4%), L-proline (7%), L-serine (4%), L-threonine (5%), L-tyrosine(4%) and L-valine (5%). A stock solution of 5 g L^{-1} was prepared in water and filter-sterilized with a 0.2-μm filter. Flasks containing media and inoculum were sealed with butyl rubber stoppers and incubated for 48 h in low light at 23°C on an orbital shaker (175 RPM, Innova 2300 Platform Shaker, Eppendorf-New Brunswick, Enfield, CT). Cells were fixed in 1% formaldehyde for 1 h at room temperature, washed 3x in 1 × PBS and stored in PBS/ethanol (40/60, vol/vol) at −20°C.

Raman microspectroscopy

Cell fractions from the ^{13}C-cellulose and D_2O soil microcosm experiments were filtered onto polycarbonate filters (GTTP type, pore size 0.2 μm, Millipore, Billerica, MA) to concentrate cells. Cells were detached from the filter (since Raman microspectroscopy cannot be performed on this material) by placing the filter into 1x PBS and vortexing for ca. 10 min at room temperature. Detached cells were pelleted by centrifugation and spotted onto an aluminum-coated slide (A1136; EMF Corporation). Raman microspectroscopy was performed using a LabRAM HR800 confocal Raman microscope (Horiba Jobin-Yvon) with a spectral resolution of 3.3 cm^{-1} using the 600 gr mm^{-1} grid and a 532-nm laser as previously described (Haider *et al.* 2010).

^{13}C-substrate incubations: spectra were obtained in the range of 300–3200 cm^{-1}. A total of 93 (from the ^{13}C-amino acids, ^{12}C-glucose) and 90 (from the ^{12}C-amino acids, ^{13}C-glucose) cell spectra from soil enrichments and more than 200 cell spectra from the ^{13}C-cellulose soil microcosm incubations were obtained using the Horiba software. These spectra were further analyzed in the range of 800–1100 cm^{-1} for a shifted phenylalanine peak (Phe) from ~1003 cm^{-1} (^{12}C-Phe) to ~964 cm^{-1} (^{13}C-Phe) upon alignment and normalization to the phenylalanine peak, followed by baselining the data. The peak area for ^{12}C-Phe (between 1000 and 1005 cm^{-1}) and ^{13}C-Phe (between 960 and 970 cm^{-1}) was calculated using an in-house script as described previously (Berry *et al.* 2015) to determine the ^{12}C-Phe to ^{13}C-Phe ratio.

D_2O incubations: a total of 38 (H_2O controls), 46 (D_2O amended) and 63 (D_2O, glucose amended) spectra were obtained from the D_2O incubations. Spectra were obtained in the range of 200–3200 cm^{-1} with the settings as described above. Spectra were aligned to the phenylalanine peak and baselined. In addition, the D_2O peaks for each spectrum were manually verified. The degree of D substitution in C–H bonds (%CD) was calculated

from the C-D peak (between 2040 and 2300 cm^{-1}) and the C-H peak (between 2800 and 3100 cm^{-1}) areas following CD/(CH+CD), all done using an in-house script and manually verified as described previously (Berry *et al.* 2015).

Filter surface analysis with scanning electron microscopy (SEM)

Sections of filters were mounted on SEM Pin Stubs (12 mm diameter, Philips, Amsterdam, Netherlands) and were gold-coated using an Agar 108 sputter coater (Agar Scientific, Essex, UK). Pictures were obtained on a Philips FEI XL 30 environmental scanning electron microscope using an acceleration voltage of 12 kilo volt (kV) at the Core Facility for Cell Imaging and Ultrastructure Research of the University of Vienna.

RESULTS

The developed sample preparation workflow for NanoSIMS and Raman microspectroscopy of soil microorganisms can be found in Fig. S1 (Supporting Information). The overarching goal was to generate a concentrated cell fraction with a considerably reduced soil particle load for efficient single-cell analyses. To that end, a procedure was tested that combined cell detachment from soil particles using either physical or chemical separation methods, separation of cells and particles via Nycodenz gradient centrifugation and subsequent filtration of the cell fraction.

Recovery of cells from soils treated with different cell detachment methods

Total recovered cells from soils that were fixed with formaldehyde (a fixation treatment typical for subsequent single-cell analyses such as FISH) across four tested cell detachment treatments ranged from 5.4×10^8 to 1.8×10^9 cells (g dry wt soil) $^{-1}$ in a beech forest soil (Klausen-Leopoldsdorf) and 1.0×10^9 to 2.1×10^9 cells (g dry wt soil) $^{-1}$ in an alpine meadow soil (Neustift) (Fig. 1). The treatment that combined the use of pyrophosphate, Tween 20 and PVP ('combination treatment') yielded the best recovery for the beech forest soil and for the alpine meadow soil (Fig. 1). However, with the exception of the 'combination treatment' compared to sonication ($P < 0.02$) in the beech forest soil no statistically significant differences among cell detachment treatments were observed. For comparison, cell counts on the beech forest soil without cell detachment treatment and Nycodenz density gradient centrifugation yielded ca. 6.0×10^8 cells (g dry wt soil) $^{-1}$. These estimates were lower than estimates with cell detachment treatment, presumably due to the high soil particle load making it challenging to obtain reliable DAPI cell counts.

When the same cell detachment treatments were applied to unfixed soil samples (as typically used for approaches based on nucleic acid extraction), they yielded slightly lower cell recoveries as compared to the formaldehyde-fixed samples, which likely reflects higher rates of cell lysis in the unfixed samples (Fig. 1). Significant differences in cell recovery between formaldehyde-fixed and unfixed samples were detected in the 'combination treatment' (beech forest soil, $P < 0.002$; alpine meadow soil, $P < 0.004$) and Tween 20 treatment (beech forest soil, $P < 0.008$). Across the unfixed samples, the 'combination treatment' yielded significantly higher numbers than the Tween20 treatment ($P < 0.04$) in the beech forest soil.

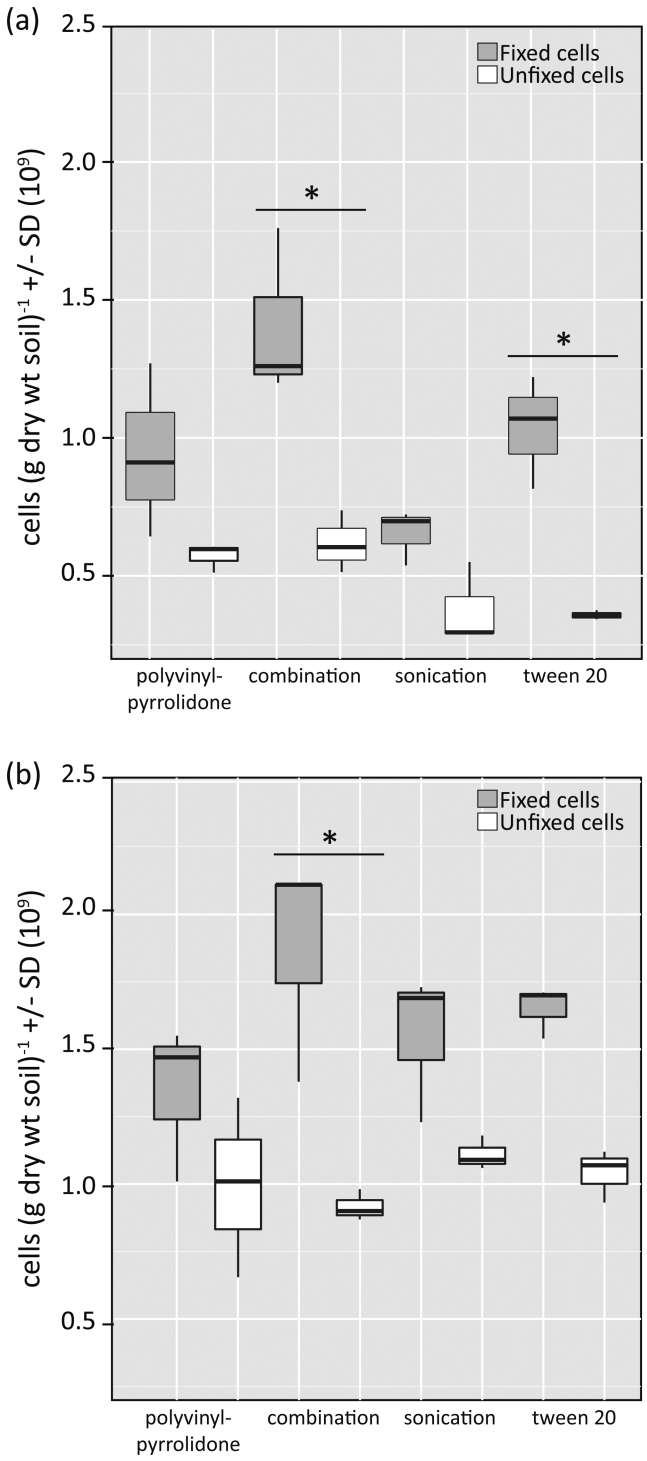

Figure 1. Box plot diagram of recovered cells (g dry wt soil) $^{-1}$ based on DAPI staining across the tested cell detachment treatments ($n = 3$ per treatment) for Klausen-Leopoldsdorf (beech forest soil) (panel **a**) and Neustift (alpine meadow soil) (panel **b**). Gray box plots represent initially formaldehyde-fixed samples, whereas white box plots represent unfixed cells. Significant differences ($p < 0.05$) in cell recovery between formaldehyde-fixed and unfixed samples are depicted with an asterisk.

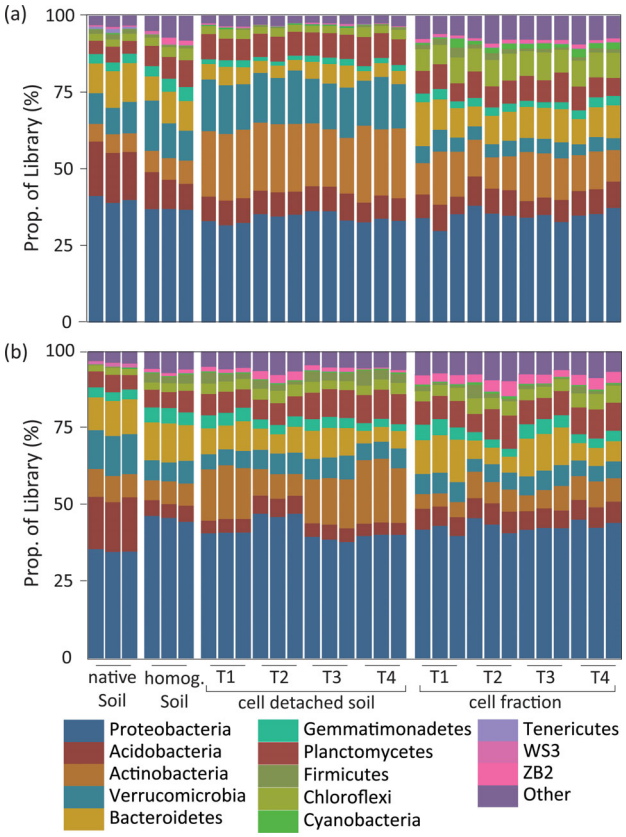

Figure 2. Relative abundance of dominant phyla based on 16S rRNA gene amplicon sequencing for Klausen-Leopoldsdorf (beech forest soil) (panel **a**) and Neustift (alpine meadow soil) (panel **b**). Biological replicates are depicted for each treatment (T1 = PVP, T2 = combination, T3 = sonication and T4 = Tween20).

Effect of developed sample preparation procedure on community structure of soil microorganisms

To assess the effect of the sample preparation procedure on the microbial community composition, the initially unfixed soil samples were investigated given the potential biases with DNA isolation associated with formaldehyde-fixed cells (Hayat 2000; Yilmaz *et al.* 2010). At different stages in the cell extraction protocol (Fig. S1, Supporting Information), 16S rRNA gene amplicon sequencing was performed on triplicate samples—(1) the starting sieved soil ('native soil'); (2) soil resuspended in PBS buffer ('homogenized soil'); (3) soil slurry after different cell detachment treatment ('cell detached soil') and (4) cell fraction after Nycodenz density gradient centrifugation ('cell fraction').

The four tested cell detachment treatments (PVP, 'combination', sonication, Tween20) had similar effects on the microbial community at the phylum level for both soil types (Fig. 2). The dominant phyla across all samples were the most abundant phyla typically recovered from molecular surveys of soils (Lauber *et al.* 2009). Across the procedure, certain phyla were either over- or underrepresented in the final 'cell fraction' as compared to the 'native soil' across both soil types (Fig. 2). For example, in the beech forest soil (Fig. 2a), the relative proportion of acidobacteria was on average 17% ('native soil'), 10% ('homogenized soil'), 8% ('cell detached soil') and 8% ('cell fraction'); of actinobacteria 6% ('native soil'), 7% ('homogenized soil'), 22% ('cell detached soil') and 13% ('cell fraction'); and of verrucomicrobia 10% ('native soil'), 12% ('homogenized soil'), 16% ('cell detached soil') and 5% ('cell fraction'). In the alpine meadow soil (Fig. 2b) for example, the relative proportion of acidobacteria was 17% ('native soil'), 5% ('homogenized soil'), 5% ('cell detached soil') and 6% ('cell fraction'); of verrucomicrobia 13% ('native soil'), 7% ('homogenized soil'), 6% ('cell detached soil') and 6% ('cell fraction'); and of firmicutes 0.3% ('native soil'), 3% ('homogenized soil'), 3% ('cell detached soil') and 1% ('cell fraction'). Significant differences ($P < 0.004$, corrected p-value for multiple comparisons) were noted between the 'native' and final 'cell fraction' relative abundances for the proteobacteria, acidobacteria, chloroflexi, cyanobacteria, planctomyces, verrucomicrobia and zb2 across both soil types, ws2 in the alpine meadow soil and actinobacteria in the beech forest soil.

Changes in the degree of recovered microbial diversity and richness across the different procedure steps were analyzed at rarified sequencing depth (OTU_{97}, Table S4, Supporting Information). In both soils, richness and diversity estimates increased in the 'homogenized soil' samples. In the alpine meadow, soil richness and diversity remained on this level up to the final 'cell fraction', while in the beech forest soil a slight decrease was observed in the 'cell detached soil' community and again an increase in the final 'cell fraction'. Changes in richness and diversity were also evaluated within specific phyla. In the beech forest soil, some phyla follow the described overall trend, while in other phyla a steady increase in diversity and richness along the procedure can be found (Table S5, Supporting Information). The above-described overall trend in the alpine meadow soil was found in the five most abundant phyla, whereas the diversity and richness seem to decrease along the procedure in lower abundant phyla (Table S6, Supporting Information).

The similarity of the 16S rRNA gene amplicon libraries generated from different stages of the cell separation and concentration procedure for the beech forest and alpine meadow soil were assessed using the Bray–Curtis distance measure and visualized using agglomerative hierarchical clustering (Fig. 3). With a few exceptions, triplicates of the same treatment clustered together. The microbial communities of the 'homogenized soil', the 'cell detached soil' and the final 'cell fraction' samples were all distinct from the 'native soil' for both soil types. This distinction of the 'native soil' from the other samples indicates that already the homogenization step influenced community structure. To test whether this pattern distinctness was due to noise (low abundant OTUs), the data were systematically reanalyzed excluding low abundant OTUs (retaining OTU_{97} clusters with a relative abundance of >0.0005% up to >0.5%). The described relationship was still observed even upon excluding OTUs with a relative abundance of <0.05% illustrating that this pattern was not caused by low abundant OTUs (data not shown). For the sake of completeness, the microbial community structure of beech forest soil samples that were initially formaldehyde fixed was also analyzed. These data can be found in Data S2 and Fig. S2 (Supporting Information).

When investigating the function of uncultured microorganisms by NanoSIMS or Raman microspectroscopy, microbial target groups are commonly stained by FISH (Wagner *et al.* 2006; Huang *et al.* 2007; Eichorst and Woebken 2014). Applying this approach to soil ecosystems with their vast diversity of microorganisms, typically FISH probes targeting a specific phylum, family or genus are utilized. Thus, we examined the sequence data in the 'native soil' and final 'cell fraction' in conjunction with the detection limit for FISH (at least 0.1% relative abundance for reliable detection; Amann and Fuchs 2008) to evaluate whether the procedure had an effect on the detectability of groups within these aforementioned taxonomic

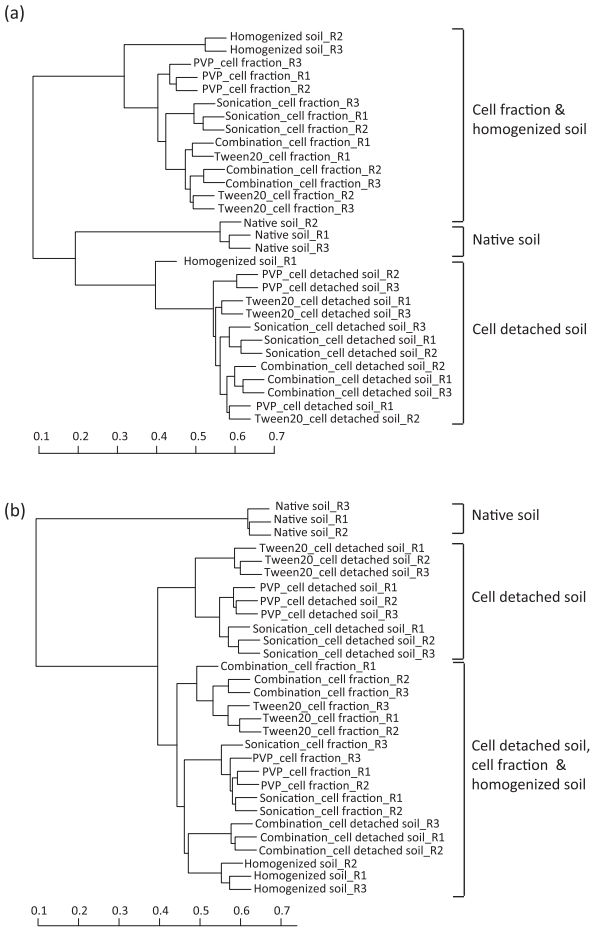

Figure 3. Agglomerative hierarchical cluster dendrogram of triplicate microbial communities of 'native soil', 'homogenized soil', 'cell detached soil' and 'cell fraction' samples from Klausen-Leopoldsdorf soil (beech forest soil) (panel **a**) and Neustift soil (alpine meadow soil) (panel **b**) based on the Bray–Curtis distance. Scale bar indicates the similarity of the communities.

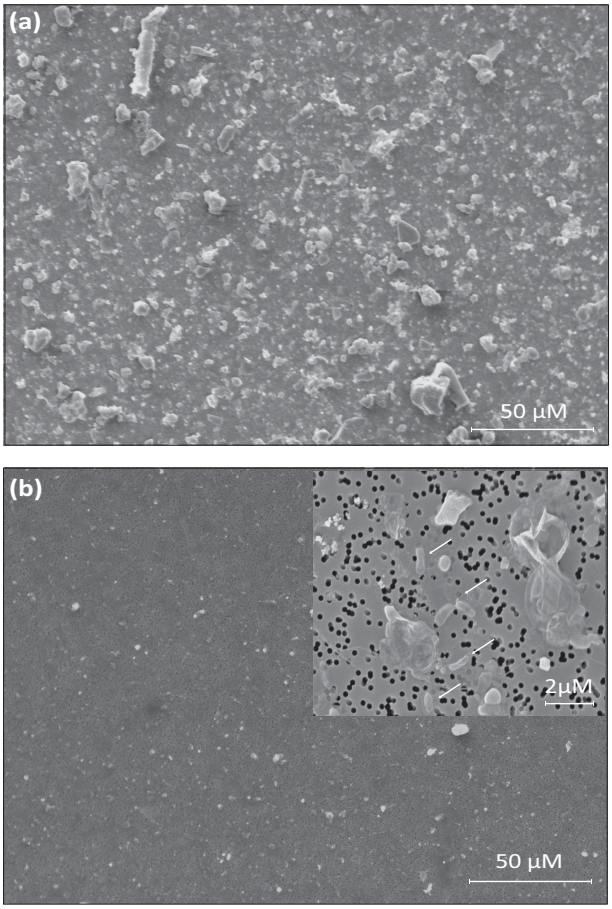

Figure 4. SEM images of polycarbonate filters carrying an untreated soil sample exhibiting copious amounts of soil particles (panel **a**), whereas a Nycodenz-treated soil sample exhibited low soil particle load (panel **b**). Inlet in panel b represents a higher magnification image depicting cells (arrows) on the filter surface. The untreated soil had to be diluted 1:100 compared to the amount of soil in the 'cell fraction' so it was possible to be imaged by SEM due to the high load of particles.

levels (Tables S7 and S8, Supporting Information). In the beech forest soil, two phyla were present in the 'native soil' but not in the final 'cell fraction'; however, seven additional phyla were detected in the final 'cell fraction' which were previously not detectable in the 'native soil'. A similar pattern was observed at the family and genus level (Table S7, Supporting Information). The alpine meadow soil showed a similar trend: two phyla were present in the 'native soil' but not in the final 'cell fraction', and seven additional phyla were detected in the final 'cell fraction' that were not detectable in the 'native soil' (Table S8, Supporting Information). This general pattern was further observed when the data were analyzed at the family and genus level and was not unique to a particular taxonomic group. For example, five families and five genera in the acidobacteria were no longer detectable in the final 'cell fraction', but were present in the 'native soil'. Yet, 14 families and 32 genera in the proteobacteria were detected above 0.1% relative sequence abundance in the final 'cell fraction', but not in the 'native soil'.

Cell detachment/concentration procedure from soil generates a cell fraction applicable for NanoSIMS analysis

The sample preparation procedure of cell detachment and concentration generated a cell fraction with strongly reduced soil particle load and concentrated cells facilitating NanoSIMS analysis. Figure 4a depicts a scanning electron micrograph of an untreated soil sample on a filter containing large soil particles (up to 50 μm) (an aliquot of soil slurry from the 'homogenized soil' stage), and Fig. 4b depicts a filter containing an aliquot of the 'cell fraction' that was attained using the 'combination treatment' in conjunction with a Nycodenz density gradient. Furthermore, the cells in the fraction were sufficiently concentrated for subsequent single-cell analysis (Fig. 4b, inlet). This cell detachment/concentration method was applied in combination with NanoSIMS to detect cellulose-responsive and N_2-fixing cells in soil microcosms incubated with stable isotope-labeled substrates (^{13}C-UL-cellulose and $^{15}N_2$, respectively). Figure 5a and b depicts single cells enriched in ^{13}C stemming from the utilization of ^{13}C-cellulose with isotope label contents ranging from 11.2 to 54.7 at%, and Fig. 5c and d ^{15}N-enriched cells from $^{15}N_2$ microcosms, with label contents ranging from 14.3 to 40.9 at%. Recent work suggested that sample preparation could have a potential dilution effect on the isotopic composition of single cells (Musat *et al.* 2014; Woebken *et al.* 2015). As such, the potential of ^{12}C contamination from Nycodenz (a derivative of

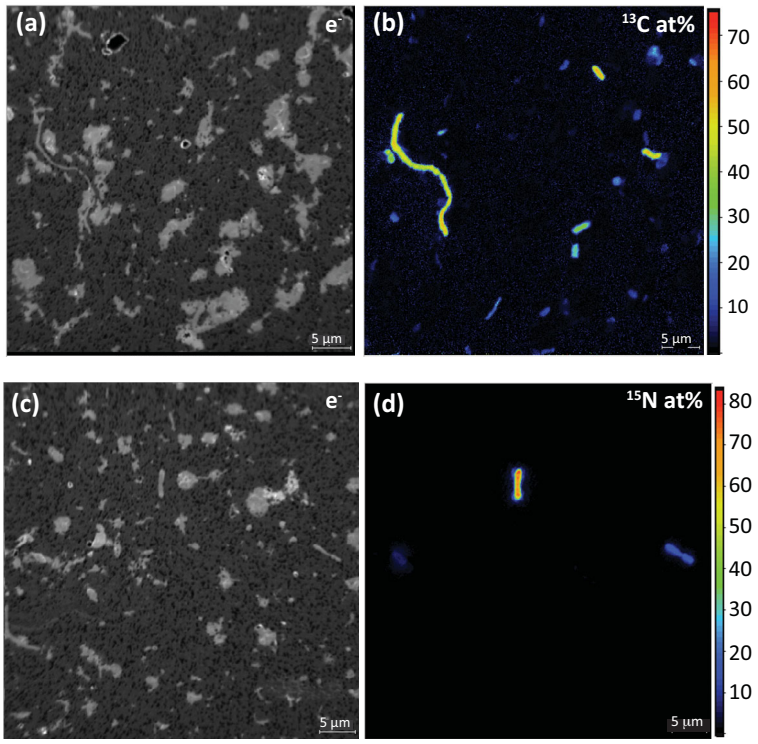

Figure 5. Single-cell isotope measurements of cells extracted from soil microcosms amended with stable isotope-labeled substrates by NanoSIMS. Panels **a** and **b**: secondary electron (e^-) and carbon isotope composition ($^{13}C/(^{12}C + ^{13}C)$, given in at%) images of cells from soil microcosms amended with ^{13}C-UL-cellulose. Microcosms were incubated for a 15-day period. Images depict single cells enriched in ^{13}C stemming from the utilization of ^{13}C-UL-cellulose. Panels **c** and **d**: secondary electron (e^-) and nitrogen isotope composition ($^{15}N/(^{14}N + ^{15}N)$, given in at%) images of cells from soil microcosms incubated with $^{15}N_2$ gas for 21 days. Images depict single cells enriched in ^{15}N stemming from nitrogen fixation of $^{15}N_2$ gas.

benzoic acid) was tested on pure cultures and did not significantly decrease their isotope enrichment (data not shown).

Cell detachment/concentration procedure from soil generates a cell fraction applicable for Raman microspectroscopy

The developed sample preparation procedure generated a cell fraction that was applicable for Raman microspectroscopy, as typical spectra for microbial cells were obtained that contained for example the characteristic peaks for phenylalanine (1003 cm^{-1}), C–H bonds and glycogen (Fig. S3, Supporting Information). The applicability of Raman microspectroscopy to detect ^{13}C-enriched cells from the conducted ^{13}C-cellulose soil microcosm experiments was tested using the characteristic ^{13}C-phenylalanine peak at 964 cm^{-1} (in contrast to the ^{12}C-phenylalanine peak at 1003 cm^{-1}; Huang *et al.* 2004). Based on NanoSIMS analysis of the same sample, soil microorganisms incorporated ^{13}C, ranging from 11.2 to 54.7 at%, from ^{13}C-cellulose into biomass. With this, their enrichment was clearly above the published detection limit of ^{13}C-enrichment levels in bacterial cells by Raman microspectroscopy (ca. 10 at%, Huang *et al.* 2007). However, the analysis of more than 200 soil cells across different treatments by Raman microspectroscopy did not reveal any cell with a detectable ^{13}C-phenylalanine peak at 964 cm^{-1} (data not shown). The phenylalanine peak shift in labeled cells will only occur if these cells synthesize phenylalanine from ^{13}C-carbon. However, soil environments can be a source of this amino acid (Monreal and McGill 1985; Jones, Owen and Farrar 2002). Thus, soil microorganisms capable of importing this amino acid might have no requirement to synthesize it. To explain the absence of microorganisms with ^{13}C-labeled phenylalanine in our analysis, we hypothesized that the microorganisms in the analyzed soil sample were preferentially taking up soil phenylalanine as compared to synthesizing it from ^{13}C-carbon arising from the provided ^{13}C-cellulose.

To test this hypothesis, soil cells (separated from the majority of the soil particles according to the PVP treatment) were incubated at defined varying concentrations of amino acids (1, 0.1, 0.001, 0.0001 and 0 g L^{-1}) and a constant concentration of glucose (10 mM). When soil cells were incubated with ^{13}C-amino acids at concentrations of 0.0001 or 0.0 g L^{-1} together with ^{12}C-glucose, the ^{12}C-phenylalanine peak at 1003 cm^{-1} was observed suggesting the cells were synthesizing phenylalanine from glucose uptake and oxidation (Fig. 6a). When ^{13}C-amino acid concentrations were higher (ranging from 0.001 to 1 g L^{-1}) in the presence of ^{12}C-glucose, a ^{13}C-phenylalanine peak at 964 cm^{-1} was typically observed suggesting that cells were incorporating the ^{13}C-labeled phenylalanine from the surrounding environment or that they were growing on imported labeled amino acids and synthesized the phenylalanine from building blocks produced during amino acid catabolism. Under these conditions, a negative relationship was observed between the ratio of the ^{12}C-phenylalanine peak (1003 cm^{-1}) to the ^{13}C-phenylalanine peak (964 cm^{-1}) and amino acid concentration (Fig. 6b). The complimentary experiment with defined varying concentrations of ^{12}C-amino acids and ^{13}C-glucose exhibited the opposite pattern. The ^{13}C-phenylalanine peak at 964 cm^{-1} was typically observed at ^{12}C-amino acid concentrations ranging from 0 to 0.1 g L^{-1}, while the ^{12}C-phenylalanine peak at 1003 cm^{-1} was observed at amino acids concentration greater than 0.001 g L^{-1}

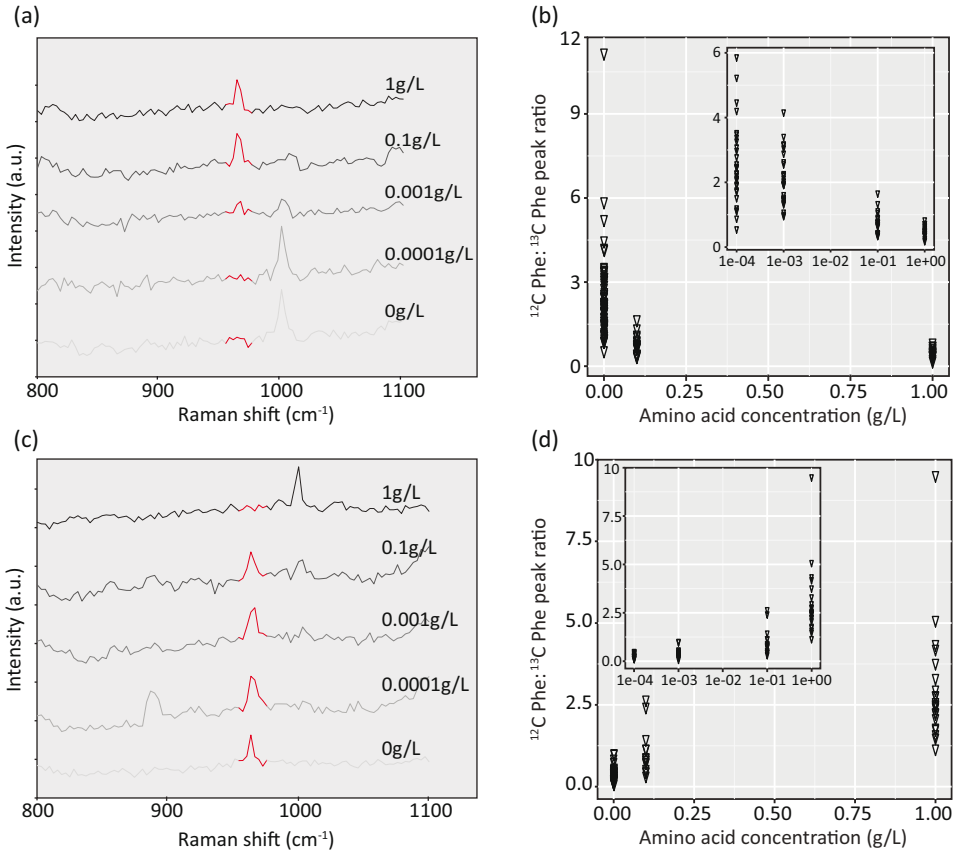

Figure 6. Raman spectra from soil microorganisms as a function of different added amino acid concentrations, ranging from 0 to 1.0 g L^{-1}. Representative Raman spectra from soil microorganisms incubated in the presence of varying ^{13}C-labeled amino acid concentrations and ^{12}C-glucose (panel **a**) and varying ^{12}C-labeled amino acid concentration and ^{13}C-glucose (panel **c**). Red regions in panels a and c depict the ^{13}C-phenylalanine peak region around 964 cm^{-1}. Panels **b** and **d** depict the ratios of phenylalanine peak area associated with ^{12}C-carbon [peak calculated between wavenumbers 1000–1005 (cm^{-1})] and ^{13}C-carbon [peak calculated between wavenumbers 960–970 (cm^{-1})] from these respective incubations. Each triangle represents a Raman spectrum of one cell. Graphical inlets depict the relationship when plotted on the log scale.

(Fig. 6c). A positive relationship was observed between the ratio of ^{12}C-phenylalanine peak (1003 cm^{-1}) to ^{13}C-phenylalanine peak (964 cm^{-1}) and amino acid concentration (Fig. 6d). In the conducted experiment, the transition between amino acid uptake and phenylalanine synthesis from glucose was at amino acid concentrations of 0.001 and 0.1 g L^{-1}.

The applicability of detecting deuterium-incorporating soil cells from heavy water (deuterium oxide, D_2O) by Raman microspectroscopy was tested through D_2O-soil microcosm experiments with and without carbon supplement. After cell extraction using the developed protocol, a broad peak was observed in the Raman spectra of cells incubated with D_2O between 2040 and 2300 cm^{-1} (Fig. 7a), presumably the C-D_x bond from newly synthesized lipids (Berry *et al.* 2015), in addition to the C-H peak (between 2800 and 3100 cm^{-1}). The degree of D substitution in C-H bonds (%CD) was calculated and compared between cells from soil microcosms incubated with D_2O only and with D_2O and an additional carbon source. In soil without supplemented carbon, 30% of the cells incorporated deuterium from D_2O above the determined threshold for considering them labeled (Fig. 7b). With supplemented carbon, this number increased to 57% of the soil microbial cells (Fig. 7b). The %CD in labeled cells from soil incubated with D_2O only ranged between 3.32 and 9.11, while 44% of the labeled cells from the incubation with supplemented carbon were highly active (>10%CD, range 3.18–29.84 %CD).

DISCUSSION

Nycodenz gradients in combination with cell detachment methods have previously been used to obtain microbial cell fractions from soil amenable for cultivation, DNA extraction and/or FISH applications (Lindahl 1996; Barra Caracciolo *et al.* 2005; Bertaux *et al.* 2007; Morono *et al.* 2013). The effect of such sample preparation has been evaluated by counting the total recovered cells by staining methods (such as DAPI and AODC) (Lindahl and Bakken 1995), typically in one soil type. This study expands upon these results by evaluating total recovery in combination with community structure analysis across the four steps of the described procedure for two different soil types. All tested cell detachment treatments yielded similar cell recoveries comparable to previously reported numbers from different soil samples (ranging from ca. 4×10^7 to 2×10^9 cells (g wt soil) $^{-1}$) (Whitman, Coleman and Wiebe 1998), with the 'combination treatment' resulting in slightly higher yields than the other treatments (Fig. 1). The developed soil sample preparation procedure can also be applied for Fluorescence Activated Cell Sorting of the extracted cells for whole genome sequencing, as the tested physical and chemical cell detachment methods of unfixed soil samples recovered a considerable portion of the starting microbial community (Fig. 1, white box plots). For such an application, it is recommended to use non-formaldehyde fixed cells (Rinke *et al.* 2014). However, when comparing the recovery of cells from

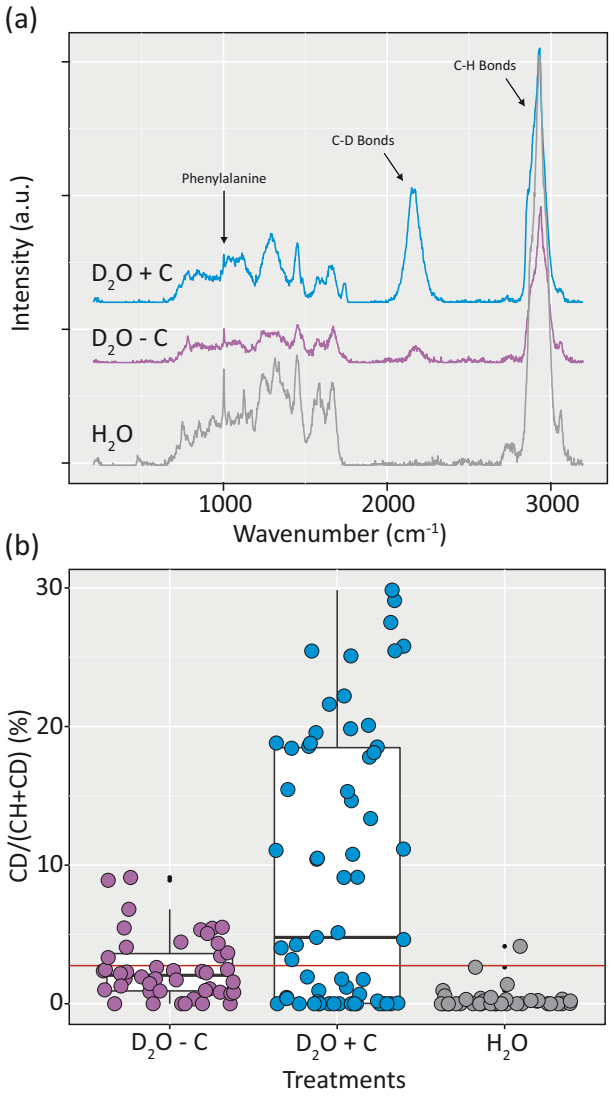

Figure 7. D_2O incubations to monitor activity of soil microorganisms in the presence and absence of glucose as an additional energy and carbon source in soil microcosm experiments. Panel **a**: representative Raman spectra of soil microorganisms incubated with D_2O and glucose (blue spectrum), D_2O without carbon source (purple spectrum) and the water (H_2O) control (gray spectrum). Panel **b**: intensity of deuterium incorporation in randomly selected soil cells incubated in the presence of D_2O, with (blue) and without (purple) glucose, measured by %CD. The control values for the H_2O incubated cells are depicted in gray. The red horizontal line depicts the threshold for a D_2O-labeled soil cell calculated based on the H_2O control values (2.75 %CD, mean + 3 SD of % CD).

initially formaldehyde-fixed and unfixed soils, significant differences were detected in cell detachment treatments that included a detergent. This suggests that including detergents in the cell detachment treatment of unfixed soil samples might lead to cell lysis at this procedure step and that treatments without detergents might be advantageous for these applications.

Previous investigations documented shifts in the bacterial community upon Nycodenz extractions as compared to the starting, native community (Courtois *et al.* 2001; Maron *et al.* 2006; Holmsgaard *et al.* 2011). Here we illustrated that each stage of the protocol appears to have an effect on the microbial community composition as assessed by 16S rRNA gene amplicon libraries (Figs 2 and 3). At the rarified sequencing depth, richness and diversity estimates increased in the 'homogenized soil' samples in both soils compared to the 'native soil', suggesting that homogenization could have weakened cell walls of some taxa and facilitate cell lysis or that when cells were attached to soil particles DNA extraction was less efficient. The steps after homogenization seem to have varying effects on richness and diversity estimates in different soils and different phyla with no definite pattern. An over- or underrepresented bacterial phyla bias was observed (Fig. 2) as documented previously (Portillo *et al.* 2013), and is believed to be a result of or a combination of (1) differential removal of cells during centrifugation with Nycodenz due to different cell densities (Laflamme *et al.* 2005), (2) tendency of certain phyla to be more closely associated with soil particles (Sessitsch *et al.* 2001), (3) differential cell lysis during the procedure, (4) PCR bias and/or (5) differential DNA extraction efficiency across the procedure (for example, extraction efficiency between 'native soil' and the final 'cell fraction'). Although higher concentrations of Nycodenz were utilized in this study (1.42 g mL^{-1}) than in previous studies (Barra Caracciolo *et al.* 2005; Holmsgaard *et al.* 2011), we still observed this over- or underrepresented bacterial phyla bias, suggesting that higher concentration of Nycodenz is not the sole culprit in this bias.

In both soils, the microbial community of the final 'cell fraction' samples all clustered together, regardless of the cell detachment treatment, and was distinct from the 'native soil' (Fig. 3). Although these compositional differences suggest that the procedure can alter the sampled microbial community, further sequence analysis demonstrated that the procedure can even improve the detectable of various phyla, families and genera when compared to the 'native soil' (Tables S7 and S8, Supporting Information). At a relative abundance cut-off of $\geq$ 0.1% (the previously described detection limit for single-cell methods; Amann and Fuchs 2008), the procedure resulted in both a gain and loss of phyla, families and genera across multiple taxonomic groups. This observation was not unique to one soil type, but found in both investigated soils, suggesting that this may be a common feature of the procedure. Interestingly, the procedure caused more gain of detectable groups in the final 'cell fraction' than loss of them suggesting that the procedure can increase the detectability of certain taxonomic groups (Tables S7 and S8, Supporting Information).

NanoSIMS and Raman microspectroscopy allow for the assessment of the targeted function at the single-cell level, and reveal community and population heterogeneity regarding the investigated activity. SIMS is a destructive technique that uses a high-energy primary ion beam to sputter small volumes of the sample material from the target surface forming the secondary ion beam with the characteristic isotope composition of the target area which can be analyzed by their mass-to-charge ratio in a mass spectrometer (Benninghoven and Rudenauer 1987). With this, NanoSIMS is sensitive to topographical unevenness and this together with the potential bias of label dilution due to redeposition of sputtered material requires the removal of large soil particles. Furthermore, this high lateral resolution analysis will only investigate a comparably small sample volume and therefore a concentrated cell fraction should be obtained for efficient analysis. Raman microspectroscopy also requires freely exposed cells to retrieve reliable cell spectra, and both techniques have not been applied yet to investigate the *in situ* function of a targeted microbial population in soils, presumably due to the high load of particles and the disperse distribution of microbial cells in soils.

We developed a sample preparation strategy (Fig. S1, Supporting Information) including cell detachment, separation from particles and subsequent cell concentration that generated a

concentrated cell fraction (Fig. 4) applicable for NanoSIMS and Raman microspectroscopy (Fig. 5 and Fig. S3, Supporting Information). With this method, we were able to successfully visualize via NanoSIMS cellulose-responsive as well as diazotrophic cells from soil microcosm experiments from the beech forest soil. The generated microbial cell fraction was also suitable for subsequent analysis via Raman microspectroscopy—indicative spectra for microbial cells were observed in both ^{13}C-substrate and D_2O incubations.

Unexpectedly and in contrast to the NanoSIMS results, no ^{13}C-labeled cells were detected by Raman microspectroscopy in the cells retrieved from the ^{13}C-cellulose soil microcosm experiment. The applicability of utilizing the characteristic phenylalanine 'red shift' to detect ^{13}C-enriched cells by Raman microspectroscopy (Huang *et al.* 2004, 2007) relies on the principle that the cell must synthesize phenylalanine *de novo* from the supplied ^{13}C-substrate. If the environmental sample contains extracellular phenylalanine of a certain concentration as well as microbes capable of importing this amino acid (or peptides) in order to fully satisfy their demand, the applicability of this approach could become limited. Our data suggest that when background amino acids (including phenylalanine) are available at a concentration higher than ca. 0.001 to 0.1g L^{-1} (ca. 0.29 to 29 μM), at least some soil microorganisms will take up those amino acids from the environment (Fig. 6) and either use them for protein biosynthesis and/or growth. If these microorganisms also participate in the degradation of ^{13}C-labeled cellulose, this would be overlooked by Raman microspectroscopy. Amino acid-, peptide- and protein-nitrogen comprise the largest fraction of identifiable organic nitrogen-containing compounds in soils. The concentration of free amino acids in soil ranges from 0 to 158 μM (Monreal and McGill 1985; Kielland 1994; Raab, Lipson and Monson 1999; Jones *et al.* 2005), and of individual amino acids from 0.01 to 50 μM although the flux of the amino acid pool can be rapid (Kielland 1995; Jones and Kielland 2002; Jones *et al.* 2009). Phenylalanine has been reported to be an abundant amino acid across many soil types (Kelley and Stevenson 1996; Martens and Loeffelmann 2003). Thus, the applicability of the characteristic phenylalanine 'red shift' to detect ^{13}C-enriched cells by Raman microspectroscopy in soil samples might be highly variable due to the ranging concentrations of amino acids in soil, together with potentially differing Kms of microorganism for amino acid uptake.

Recently, it was documented that incorporation of D from heavy water into cellular biomass can be used as a general activity marker for experiments with microbial pure and mixed cultures (Berry *et al.* 2015), a principle we wanted to evaluate for its applicability to soil microorganisms. D_2O can be used as a general activity marker, since in all known lipid biosynthesis pathways hydrogen from water is incorporated during the reductive steps of fatty acids synthesis (Zhang, Gillespie and Sessions 2009). In addition, the use of D_2O as compared to ^{13}C- or ^{15}N-labeled substrates can be advantageous for studying the *in situ* ecophysiology of uncultured microorganisms, as it does not change the environmental substrate pool. In soil microcosms with D_2O but without supplemented energy and carbon source, 30% of the cells were D labeled and considered active (Fig. 7b), which corresponds to previous estimations of active bacterial and archaeal cells in soil (ca. 20 %; Jones and Lennon 2010). In contrast, ca. 2-fold more cells (57%) were detected as active in incubations with D_2O together with glucose as an energy and carbon source. And 44% of those cells were highly active with %CD values between 10 and 29%, whereas the highest %CD without supplemented carbon was 9%. All in all, using the incorporation of D from D_2O into lipids as a general or substrate-specific activity assay was successfully applied to soil microorganisms and can be a very valuable addition for ecological studies of soil microbes in particular if combined with FISH.

CONCLUSION

We have developed and evaluated a sample preparation procedure for soils that generates a microbial cell fraction with high cell density and reduced particle load for the application of single-cell analysis methods, such as NanoSIMS and Raman microspectroscopy. 16S rRNA gene amplicon sequencing of samples taken at various steps of the developed procedure showed that – as expected – changes in the community structure occur during application of the protocol. However, analysed at different taxonomic levels (phylum, family and genus) going from the 'native soil' to the concentrated 'cell fraction' leads to loss as well as gain in groups above the detection limit. In combination with stable isotope incubations, this procedure allows an efficient analysis of microbial activity at the single-cell level in soil systems and can be applied to the investigation of major microbial driven processes within the terrestrial C and N cycle. Preliminary data indicate that this procedure is also applicable to other terrestrial samples such as sandy soil crusts and peatland soil (data not shown). Furthermore, the procedure can be applied to unfixed soil samples, and thus could be used in single-cell sequencing approaches, such as single-cell sorting combined with subsequent whole genome amplification. In conclusion, the described sample preparation pipeline enables the efficient investigation of microbial activities in soil samples at the single-cell level by NanoSIMS and Raman microspectroscopy, but should also facilitate single-cell sorting and sequencing of soil microorganisms. We believe that these advancements will continue to bridge the knowledge gap between the uncultivated majority and their function in soil environments.

SUPPLEMENTARY DATA

Supplementary data are available at FEMSEC online.

ACKNOWLEDGEMENTS

We would like to thank Susannah Tringe, Tijana Glavina Del Rio, Stephanie Malfatti, and Michael Barton of the Joint Genome Institute for their assistance in obtaining and processing iTag sequence data. We would like to thank Irene Lichtscheidl-Schultz at the Core Facility Cell Imaging and Ultrastructure Research for her assistance with the electron micrographs. We thank the United States Department of Agriculture for supplying the *Chaetomium globosum* strain. The authors would like to thank Andreas Richter and Lucia Fuchslueger for their assistance with soil collection and Marton Palatinszky, Markus Schmid and Roey Angel for their assistance with the Raman microspectroscopy data analysis.

FUNDING

This work was supported by a Marie Curie International Incoming Fellowship [300807 to S.A.E.], a Marie Curie Career Integration Grant [321742 to D.W.], an Austrian Science Fund FWF project grant [P25700-B20 to D.W.] and an ERC Advanced grant [NITRICARE, 294343, to M.W.]. The work conducted by the U.S. Department of Energy Joint Genome Institute (JGI), a DOE

Office of Science User Facility, is supported under Contract No. DE-AC02-05CH11231. Further supported was provided by the JGI Emerging Technologies Opportunity Program.

Conflict of interest. None declared.

REFERENCES

Amann R, Fuchs BM. Single-cell identification in microbial communities by improved fluorescence in situ hybridization techniques. *Nat Rev Microbiol* 2008;**6**:339–48.

Barra Caracciolo A, Grenni P, Cupo C, *et al.* In situ analysis of native microbial communities in complex samples with high particulate loads. *FEMS Microbiol Lett* 2005;**253**:55–8.

Benninghoven A, Rudenauer F. *Secondary Ion Mass Spectrometry: Basic Concepts*. Instrumental Aspects, J. Wiley 1987.

Berry D, Mader E, Lee TK, *et al.* Tracking heavy water (D_2O) incorporation for identifying and sorting active microbial cells. *P Natl Acad Sci USA* 2015;**112**:E194–203.

Bertaux J, Gloger U, Schmid M, *et al.* Routine fluorescence in situ hybridization in soil. *J Microbiol Meth* 2007;**69**:451–60.

Caldwell BA. Enzyme activities as a component of soil biodiversity: a review. *Pedobiologia* 2005;**49**:637–44.

Caporaso JG, Lauber CL, Walters WA, *et al.* Global patterns of 16S rRNA diversity at a depth of millions of sequences per sample. *P Natl Acad Sci USA* 2011;**108**:4516–22.

Clode PL, Kilburn MR, Jones DL, *et al.* In situ mapping of nutrient uptake in the rhizosphere using nanoscale secondary ion mass spectrometry. *Plant Physiol* 2009;**151**:1751–7.

Cole JR, Chai B, Farris RJ, *et al.* The Ribosomal Database Project (RDP-II): sequences and tools for high-throughput rRNA analysis. *Nucleic Acids Res* 2005;**33**:D294–6.

Corradob G, Sanchez-Cortes S, Frandoso O, *et al.* Surface-enhanced Raman and fluorescence a joint analysis of soil humic acids. *Anal Chim Acta* 2008;**616**:69–77.

Courtois S, Frostegård A, Göransson P, *et al.* Quantification of bacterial subgroups in soil: comparison of DNA extracted directly from soil or from cells previously released by density gradient centrifugation. *Environ Microbiol* 2001;**3**:431–9.

Dekas AE, Poretsky RS, Orphan VJ. Deep-sea archaea fix and share nitrogen in methane-consuming microbial consortia. *Science* 2009;**326**:422-6.

Edgar RC, Haas BJ, Clemente JC, *et al.* UCHIME improves sensitivity and speed of chimera detection. *Bioinformatics* 2011;**27**:2194–200.

Eichorst SA, Breznak JA, Schmidt TM. Isolation and characterization of newly isolated soil bacteria that define *Terriglobus* gen. nov., in the phylum *Acidobacteria*. *Appl Environ Microb* 2007;**73**:2708–17.

Eichorst SA, Kuske CR, Schmidt TM. Influence of plant polymers on the distribution and cultivation of bacteria in the phylum *Acidobacteria*. *Appl Environ Microb* 2011;**77**:586–96.

Eichorst SA, Woebken D. Investigation of microorganisms at the single-cell level using Raman Microspectroscopy and Nanometer-scale Secondary Ion Mass Spectrometry. In: Skovhus TL, Caffrey S (eds). *Molecular Methods and Applications in Microbiology*. Norfolk, UK: Caister Academic Press, 2014;203–211.

Foster RA, Kuypers MM, Vagner T, *et al.* Nitrogen fixation and transfer in open ocean diatom-cyanobacterial symbioses. *ISME J* 2011;**5**:1484–93.

Haider S, Wagner M, Schmid MC, *et al.* Raman microspectroscopy reveals long-term extracellular activity of chlamydiae. *Mol Microbiol* 2010;**77**:687–700.

Halm H, Musat N, Lam P, *et al.* Co-occurrence of denitrification and nitrogen fixation in a meromictic lake, Lake Cadagno (Switzerland). *Environ Microbiol* 2009;**11**:1945–58.

Harz A, Roesch P, Popp J. Vibrational spectroscopy-A powerful tool for the rapid identification of microbial cells at the single-cell level. *Cytom Part A* 2009;**75**:104–13.

Hatton P-J, Remusat L, Zeller B, *et al.* A multi-scale approach to determine accurate elemental and isotopic ratios by nanoscale secondary ion mass spectrometry imaging. *Rapid Commun Mass Sp* 2012;**26**:1363–71.

Hayat MA. *Principles and Techniques of Electron Microscopy: Biological Applications*. Cambridge: Cambridge University Press, 2000.

Heister K, Hoeschen C, Pronk GJ, *et al.* NanoSIMS as a tool for characterizing soil model compounds and organomineral associations in artificial soils. *J Soils Sediments* 2012;**12**:35–47.

Herrmann AM, Ritz K, Nunan N, *et al.* Nano-scale secondary ion mass spectrometry—a new analytical tool in biogeochemistry and soil ecology: a review article. *Soil Biol Biochem* 2007;**39**:1835–50.

Holmsgaard PN, Norman A, Hede SC, *et al.* Bias in bacterial diversity as a result of Nycodenz extraction from bulk soil. *Soil Biol Biochem* 2011;**43**:2152–9.

Huang WE, Griffiths RI, Thompson IP, *et al.* Raman microscopic analysis of single microbial cells. *Anal Chem* 2004;**76**:4452–8.

Huang WE, Stoecker K, Griffiths R, *et al.* Raman-FISH: combining stable-isotope Raman spectroscopy and fluorescence in situ hybridization for the single cell analysis of identity and function. *Environ Microbiol* 2007;**9**:1878–89.

Jarvis RM, Goodacre R. Discrimination of bacteria using surface-enhanced Raman spectroscopy. *Anal Chem* 2004;**76**:40–7.

Jehlicka J, Edwards HGM, Oren A. Bacterioruberin and salinixanthin carotenoids of extremely halophilic Archaea and Bacteria: a Raman spectroscopic study. *Spectrochim Acta A* 2013;**106**:99–103.

Jones DL, Kielland K. Soil amino acid turnover dominates the nitrogen flux in permafrost-dominated taiga forest soils. *Soil Biol Biochem* 2002;**34**:209–19.

Jones DL, Kielland K, Sinclair FL, *et al.* Soil organic nitrogen mineralization across a global latitudinal gradient. *Global Biogeochem Cy* 2009;**23**:GB1016.

Jones DL, Owen AG, Farrar JF. Simple method to enable the high resolution determination of total free amino acids in soil solutions and soil extracts. *Soil Biol Biochem* 2002;**34**:1893–902.

Jones DL, Shannon D, Junvee-Fortune T, *et al.* Plant capture of free amino acids is maximized under high soil amino acid concentrations. *Soil Biol Biochem* 2005;**37**:179–81.

Jones SE, Lennon JT. Dormancy contributes to the maintenance of microbial diversity. *P Natl Acad Sci USA* 2010;**107**:5881–6.

Kaiser C, Kilburn MR, Clode PL, *et al.* Exploring the transfer of recent plant photosynthates to soil microbes: mycorrhizal pathway vs direct root exudation. *New Phytol* 2015;**205**:1537–51.

Kelley KR, Stevenson FJ. Organic forms of N in soil. In: Piccolo A (ed). *Humic Substances in Terrestrial Ecosystems*. The Netherlands: Elsevier Science, 1996.

Kielland K. Amino-acid-absorption by arctic plants - implications for plant nutrition and nitrogen cycling. *Ecology* 1994;**75**:2373–83.

Kielland K. Landscape patterns of free amino acids in arctic tundra soils. *Biogeochemistry* 1995;**31**:85–98.

Kilburn MR, Jones DL, Clode PL, *et al.* Application of nanoscale secondary ion mass spectrometry to plant cell research. *Plant Signal Behav* 2010;**5**:760–2.

Kumar V, Kampe B, Rösch P, *et al.* Characterization of carotenoids in soil bacteria and investigation of their photodegradation by UVA radiation via resonance Raman spectroscopy. *Analyst* 2015;**140**:4584–93.

Laflamme C, Ho J, Veillette M, *et al.* Flow cytometry analysis of germinating Bacillus spores, using membrane potential dye. *Arch Microbiol* 2005;**183**:107–12.

Lauber CL, Hamady M, Knight R, *et al.* Pyrosequencing-based assessment of soil pH as a predictor of soil bacterial community structure at the continental scale. *Appl Environ Microb* 2009;**75**:5111–20.

Lechene C, Hillion F, McMahon G, *et al.* High-resolution quantitative imaging of mammalian and bacterial cells using stable isotope mass spectrometry. *J Biol* 2006;**5**:20.

Lechene CP, Luyten Y, McMahon G, *et al.* Quantitative imaging of nitrogen fixation by individual bacteria within animal cells. *Science* 2007;**317**:1563–6.

Li M, Canniffe DP, Jackson PJ, *et al.* Rapid resonance Raman microspectroscopy to probe carbon dioxide fixation by single cells in microbial communities. *ISME J* 2012;**6**:875–85.

Lindahl V. Improved soil dispersion procedures for total bacterial counts, extraction of indigenous bacteria and cell survival. *J Microbiol Meth* 1996;**25**:279–86.

Lindahl V, Bakken LR. Evaluation of methods for extraction of bacteria from soil. *FEMS Microbiol Ecol* 1995;**16**:135–42.

Luna AS, Lima ICA, Rocha WFC, *et al.* Classification of soil samples based on Raman spectroscopy and X-ray fluorescence spectrometry combined with chemometric methods and variable selection. *Anal Methods* 2014;**6**:8930–9.

Magoc T, Salzberg SL. FLASH: fast length adjustment of short reads to improve genome assemblies. *Bioinformatics* 2011;**27**:2957–63.

Maron PA, Schimann H, Ranjard L, *et al.* Evaluation of quantitative and qualitative recovery of bacterial communities from different soil types by density gradient centrifugation. *Eur J Soil Biol* 2006;**42**:65–73.

Martens DA, Loeffelmann KL. Soil amino acid composition quantified by acid hydrolysis and anion chromatography-pulsed amperometry. *J Agr Food Chem* 2003;**51**:6521–9.

Milucka J, Perdelman TG, Polerecky L, *et al.* Zero-valent sulphur is a key intermediate in marine methane oxidation. *Nature* 2012;**491**:541–6.

Monreal CM, McGill WB. Centrifugal extraction and determination of free amino-acids in soil solutions by TLC using tritiated 1-fluoro-2,4-dinitrobenzene. *Soil Biol Biochem* 1985;**17**:533–9.

Moore KL, Lombi E, Zhao F-J, *et al.* Elemental imaging at the nanoscale: NanoSIMS and complementary techniques for element localisation in plants. *Anal Bioanal Chem* 2011a;**402**:3263–73.

Moore KL, Schroeder M, Wu Z, *et al.* High-resolution secondary ion mass Spectrometry reveals the contrasting subcellular distribution of arsenic and silicon in rice roots. *Plant Physiol* 2011b;**156**:913–24.

Morono Y, Terada T, Nishizawa M, *et al.* Carbon and nitrogen assimilation in deep subseafloor microbial cells. *P Natl Acad Sci USA* 2011;**108**:18295–300.

Morono Y, Terada T, Kallmeyer J, *et al.* An improved cell separation technique for marine subsurface sediments: applications for high-throughput analysis using flow cytometry and cell sorting. *Environ Microbiol* 2013;**15**:2841–9.

Mueller CW, Koelbl A, Hoeschen C, *et al.* Submicron scale imaging of soil organic matter dynamics using NanoSIMS—from single particles to intact aggregates. *Org Geochem* 2012;**42**:1476–88.

Musat N, Halm H, Winterholler B, *et al.* A single-cell view on the ecophysiology of anaerobic phototrophic bacteria. *P Natl Acad Sci USA* 2008;**105**:17861–6.

Musat N, Stryhanyuk H, Bombach P, *et al.* The effect of FISH and CARD-FISH on the isotopic composition of ^{13}C and ^{15}N labeled *Pseudomonas putida* cells measured by nanoSIMS. *Syst Appl Microbiol* 2014;**37**:267–76.

Nuccio EE, Hodge A, Pett-Ridge J, *et al.* An arbuscular mycorrhizal fungus significantly modifies the soil bacterial community and nitrogen cycling during litter decomposition. *Environ Microbiol* 2013;**15**:1870–81.

Pätzold R, Keuntje M, Theophile K, *et al.* In situ mapping of nitrifiers and anammox bacteria in microbial aggregates by means of confocal resonance Raman microscopy. *J Microbiol Meth* 2008;**72**:241–8.

Ploug H, Adam B, Musat N, *et al.* Carbon, nitrogen and O2 fluxes associated with the cyanobacterium *Nodularia spumigena* in the Baltic Sea. *ISME J* 2011;**5**:1549–58.

Portillo MC, Leff JW, Lauber CL, *et al.* Cell size distributions of soil bacterial and archaeal taxa. *Appl Environ Microb* 2013;**79**:7610–7.

Prosser JI. Replicate or lie. *Environ Microbiol* 2010;**12**:1806–10.

Raab TK, Lipson DA, Monson RK. Soil amino acid utilization among species of the *Cyperaceae*: plant and soil processes. *Ecology* 1999;**80**:2408–19.

Radajewski S, McDonald IR, Murrell JC. Stable-isotope probing of nucleic acids: a window to the function of uncultured microorganisms. *Curr Opin Biotech* 2003;**14**:296–302.

Remusat L, Hatton P-J, Nico PS, *et al.* NanoSIMS Study of organic matter associated with soil aggregates: advantages, limitations, and combination with STXM. *Environ Sci Technol* 2012;**46**:3943–9.

Rickwood D, Ford T, Graham J. Nycodenz—a new non-ionic iodinated gradient medium. *Anal Biochem* 1982;**123**:23–31.

Rinke C, Lee J, Nath N, *et al.* Obtaining genomes from uncultivatedenvironmental microorganisms using FACS–basedsingle-cell genomics. *Nat Protoc* 2014;**9**:1038–48.

Rosch P, Harz M, Schmitt M, *et al.* Chemotaxonomic identification of single bacteria by micro-Raman spectroscopy: application to clean-room-relevant biological contaminations. *Appl Environ Microb* 2005;**71**:1626–37.

Sessitsch A, Weilharter A, Gerzabek MH, *et al.* Microbial population structures in soil particle size fractions of a long-term fertilizer field experiment. *Appl Environ Microb* 2001;**67**:4215–24.

Tomic Z, Makreski P, Gajic B. Identification and spectra-structure determination of soil minerals: Raman study supported by IR spectroscopy and X-ray powder diffraction. *J Raman Spectrosc* 2010;**41**:582–6.

Vogel C, Mueller CW, Höschen C, *et al.* Submicron structures provide preferential spots for carbon and nitrogen sequestration in soils. *Nat Commun* 2014;**5**:1–7.

Wagner M. Single-cell ecophysiology of microbes as revealed by raman microspectroscopy or secondary ion mass spectrometry imaging. *Annu Rev Microbiol* 2009;**63**:411–29.

Wagner M, Horn M, Daims H. Fluorescence in situ hybridisation for the identification and characterisation of prokaryotes. *Curr Opin Microbiol* 2003;**6**:302–9.

Wagner M, Nielsen PH, Loy A, *et al.* Linking microbial community structure with function: fluorescence in situ hybridization-microautoradiography and isotope arrays. *Curr Opin Biotech* 2006;**17**:83–91.

Whitman WB, Coleman DC, Wiebe WJ. Prokaryotes: the unseen majority. *P Natl Acad Sci USA* 1998;**95**:6578–83.

Woebken D, Burow L, Prufert-Bebout L, *et al*. Identification of a novel cyanobacterial group as active diazotrophs in a coastal microbial mat using NanoSIMS analysis. *ISME J* 2012;**6**:1427–39.

Woebken D, Burow LC, Behnam F, *et al*. Revisiting N_2 fixation in Guerrero Negro intertidal microbial mats with a functional single-cell approach. *ISME J* 2015;**9**:485–96.

Yilmaz S, Haroon MF, Rabkin BA, *et al*. Fixation-free fluorescence in situ hybridization for targeted enrichment of microbial populations. *ISME J* 2010;**4**:1352–6.

Zheng L, Lee WS, Li M, *et al*. Analysis of soil phosphorus concentration based on Raman spectroscopy. *SPIE Asia* 2012; **8527**:852718.

Zhang X, Gillespie AL, Sessions AL. Large D/H variations in bacterial lipids reflect central metabolic pathways. *P Natl Acad Sci USA* 2009;**106**:12580–6.